



HAL
open science

SWEAT: Snow Water Equivalent with AlTimetry

Manuela Unterberger, Stephen Hardwick, Dries Agten, Jan J. Benninga, Carlos Diaz Schümmer, Julia Maria Donnerer, Georg Fischer, Marie Henriksen, Alexandre Hippert-Ferrer, Maryam Jamali, et al.

► **To cite this version:**

Manuela Unterberger, Stephen Hardwick, Dries Agten, Jan J. Benninga, Carlos Diaz Schümmer, et al.. SWEAT: Snow Water Equivalent with AlTimetry. EGU General Assembly, Apr 2017, Vienne, Austria. pp.2017 - 16487. hal-02184213

HAL Id: hal-02184213

<https://hal.science/hal-02184213>

Submitted on 15 Apr 2020

HAL is a multi-disciplinary open access archive for the deposit and dissemination of scientific research documents, whether they are published or not. The documents may come from teaching and research institutions in France or abroad, or from public or private research centers.

L'archive ouverte pluridisciplinaire **HAL**, est destinée au dépôt et à la diffusion de documents scientifiques de niveau recherche, publiés ou non, émanant des établissements d'enseignement et de recherche français ou étrangers, des laboratoires publics ou privés.



SWEAT

SNOW WATER EQUIVALENT WITH ALTIMETRY

TEAM ORANGE MEMBERS: *Dries Agten, Harm-Jan Benninga, Carlos Diaz Schümmer, Julia Maria Donnerer, Georg Fischer, Marie Henriksen, Alexandre Hippert Ferrer, Maryam Jamali, Stefano Marinaci, Toby Mould, Liam Phelan, Stephanie Rosker, Caroline Schrenker, Kerstin Schulze and Jorge Emanuel Telo Bordalo Monteiro*

TEAM TUTORS: *Manuela Unterberger and Stephen Hardwick*

Team Orange would like to thank FFG and ESA for organising the Summer School Alpbach 2016. Also thanks to all the tutors and lecturers guiding Team Orange towards this product, and a special thank to our team tutors.

ALPBACH SUMMER SCHOOL 2016

July 21, 2016

ABSTRACT

Snow Water Equivalent (SWE) is not directly measured by current satellite missions but has a significant impact on society and our lack of understanding contributes to significant inaccuracies in current estimations of hydrological and climate models, calculations of the Earth's energy balance (albedo) and flood predictions. To address this, the SWEAT (Snow Water Equivalent with Altimetry) mission aims to measure SWE directly on sea ice and land in the polar regions above 60° and below -60° latitude. The primary scientific objectives are to (a) improve estimations of global SWE from passive microwave products and (b) improve numerical snow and climate models. The mission will implement a novel combination of Ka- and Ku-band radioaltimeter technology, each providing different snow penetration properties. Airborne Laser altimeter campaigns will shadow the satellite orbit path early, middle and late winter for the first two years of the mission to confirm Ka-Band surface measurement accuracies. The combined difference in signal penetration results will enable more accurate determination of SWE.

1. INTRODUCTION

The water cycle involves the process where water circulates around the Earth's atmosphere, lands and oceans experiencing different physical states. To study how the water cycle changes over time, satellite and airborne remote sensing missions are typically employed. Over the last 40 years of satellite missions however, several major aspects of the water cycle still lack investigation due to the complexity of the system, especially in the cryosphere regions when measuring Snow Water Equivalent (SWE) on sea ice and land. Snow makes up the largest varying landscape feature on the Earth's surface [12], where more than 1/6 of the Earth's pop-

ulation rely on glacier and seasonal snow packs for their water supply [1]. Therefore, the accurate measurement of the snow phase of the water cycle would have a large impact on society. Current space missions exist which aim to measure the changes in sea ice using radar altimetry instruments, but their results are significantly hindered by uncertainties introduced by the snow cover on top of the sea ice.

This leads to significant inaccuracies in compensating and measuring true water inventories since the density of snow varies significantly between every measurement, and its density is significantly less than the ice they are measuring.

The lack of SWE understanding has a serious knock on effect on hydrological and climate models, calculations of the Earth's energy balance (albedo), transpolar ship navigation, global flood predictions and hydropower dams. Therefore, closing this gap in remote sensing knowledge for SWE would have a positive and significant impact on the world.

2. SNOW WATER EQUIVALENT

SWEAT is going to measure the snow water equivalent (SWE), which is the volume of water stored in a given volume of snow. The snow height h is related to SWE by the snow density ρ_s and the density of water ρ_w :

$$SWE = h \frac{\rho_s}{\rho_w}, \quad (1)$$

where height is measured in meters, density in kilograms per meter cubed and SWE is measured in m of water [36]. SWE can therefore be seen as the depth of water that would theoretically result if you melted the entire snowpack instantaneously [39].

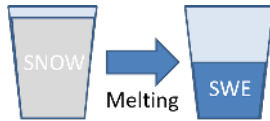


Figure 1: Illustration of the Snow Water Equivalent

2.1. AVAILABLE SWE PRODUCTS

SWE observations are currently carried out in-situ, via airborne campaigns (e.g. NASA Operation IceBridge Mission) and by space missions, such as the Advanced Microwave Scanning Radiometer - Earth Observing System (AMSR-E) sensor on NASA's Aqua satellite. Products that combine observations and modelling are ESA GlobSnow and the EUMETSAT Satellite Application Facility on Support to Operational Hydrology and Water Management (H-SAF). AMSR-E can measure SWE with an accuracy of 11 to 32 cm [?]. In-situ measurements of SWE cannot be repeated, as they are always destructive, therefore one has to rely on the accuracy of single measurements. SWEAT will close the gap between the scarce and supposedly accurate in-situ observations and global coarse-scale inaccurate observations.

3. SCIENTIFIC OBJECTIVES

3.1. 1STSCIENTIFIC OBJECTIVES

Passive microwave sensors (PM) such as SMMR, AMSR-E, and SSM/I on board satellites have the capability to provide global snow observations and provide information on SWE, a parameter which is required for various hydrological, meteorological and climatological applications and flood forecasting [22]. However, the errors associated with the passive microwave measurements of SWE have been well documented [5]. One of the major sources of uncertainty in microwave snow water estimations comes from an incomplete knowledge of determining snow grain size. Several studies [18] reveal that ice particles and snowgrains can exist in a number of highly variable and complex shapes depending on the environmental conditions they were exposed to during growth. Figure 2 shows an example of different crystal, aggregate, and snow grain shapes types.

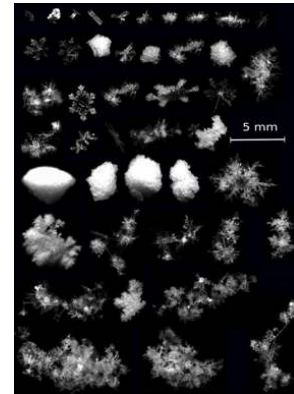


Figure 2: Example of ice and snow grain shapes (courtesy of Alexey Kljatov).

It is not feasible to know the exact shape of each snow grain. In principle, the shape of each snow grain should be known for an accurate calculation of SWE. This is therefore a major error source of SWE estimation since the models derive their values using a simplified snow grain geometry. Pullianen (2006) has shown that assimilating space-borne microwave radiometer data and ground-based observations of snow grain shapes can improve the SWE value retrieved (reader is referred to Figure 7 in [23]). However these ground-based observations are sparse. Figure 3 shows a schematic representation of a SWE retrieval model from passive microwave observation. As shown in this diagram, observations in the microwave spectral region are made and the model aims to simulate those observations. Firstly, initial assumptions of grain size are required. Then,

understanding of the relationship between microwave signals and snowpack evolution, independent from SWE. The penetration depth of the signals in this mission is important to understand since penetration bias is not entirely understood. This property is particularly important for SAR Interferometry digital elevation models (DEM) and for making mass balance estimations for glaciers and ice sheets. Therefore, there is a large demand from the scientific community to improve the microwave penetration into snow knowledge [29] [34]. The second goal is to reduce uncertainty in sea ice thickness measurements caused by uncertainties due to snow cover. Up to now, the sea ice thickness is calculated based on measurements of the free board height (the height of ice above the local sea surface level). Currently, the snow on top of this ice cannot be directly measured and thus is mitigated using snow models to provide an estimate of SWE with an accuracy of 10 cm [8]. SWEAT would improve global SWE estimations of passive microwave products, snow model accuracy and thus sea ice thickness calculations.

4. MEASUREMENT PRINCIPLES

Existing satellite missions using optical instruments only see snow from its white colour. However, this method does not provide much useful information about the quantity of snow present in a defined area. The currently operating AMSR-E SWE product relies on the microwave emission from snow which is measured using a passive microwave instrument [31]. However, this method only provides an extremely coarse resolution which inherently produces a large bias in the results due to the natural microstructure and stratification of snow producing even larger uncertainty in the SWE data. The backscatter method that underpinned the proposed CoReH2O mission is also strongly influenced by the grain size and snow layering, therefore also succumbing to the complexity limitation of snow just like passive microwave measurements [7].

In contrast, the SWEAT mission uses an altimeter which utilises an active source of microwaves in the Ka- and Ku-band, capable of penetrating into the snow microstructure and thus directly retrieves the SWE. The SWEAT mission will be the first mission to be capable of directly measuring SWE and directly get information about the snow pack on ice and land from space.

4.1. KA-BAND ALTIMETER

Unlike frequencies ranged in the X-band (8-12 GHz) and Ku-bands (12-18 GHz), Ka-band microwaves (35-37 GHz) have a maximum snow pack penetration depth

of up to 20 cm for dry snow at 37 GHz [17], but decreases to 1 cm when the water content of snow increases from 0 % to 4 % in volume [38]. That penetration depth is reduced when the snow pack is deep, stratified, winter snow [35]. Snow penetration also depends on the internal structure of snow, mainly driven by snow grain size and snow density. Penetration within a medium depends on the absorption and scattering characteristics of that medium, which are dictated directly by the wavelength used. For Ka-band ($\lambda \approx 0.8$ cm), the volume scattering of snow dominates over the scattering caused by the ice surface [40]. This volume scattering is caused by dielectric discontinuities that exist between the air and the ice within the snow pack. Based on this, the dielectric constant of dry snow can be estimated as a function of the snow density [3]. Furthermore, penetration decreases when snow grain have a more coarse surface structure. Due to all of this, current models therefore tend to overestimate depth in dry snow [28], which justifies the use of Ka-band frequency to measure the snow surface.

4.2. KU-BAND ALTIMETER

Compared to the Ka-band, Ku-band microwaves ($\lambda \approx 2$ cm) can penetrate the snow pack up to several meters as scattering decreases by a factor of 55, with penetration depths up to 15 m in high latitudes with dry snow regions [41]. Moreover, surface scattering dominates backscatter in sea ice for a space borne Ku-band radar altimeter [2]. Therefore, Ku-band microwaves are more likely to be reflected by the ice and soil surfaces.

4.3. DUAL-FREQUENCY

We present an innovative method to measure the SWE by using a nadir-looking altimetry principle in the Ka- and Ku-bands. Overall, SWE equals the product of snow height h and its bulk density ρ . Similarly, the travel time t of an electromagnetic signal through a snow pack equals the product of the snow height h and its refractive index n , shown in eq. 4. By employing a multifrequency altimeter in space, this mission aims to retrieve altimetry measurements from the snow surface and the snow-ice or snow-ground interface below the snow pack simultaneously. The travel time difference Δt between the snow surface return and the return from below the snow pack is then:

$$\Delta t = h \cdot n \quad (4)$$

Since the signals from the altimeters have different snow penetration capabilities, the mission will be able

to directly measure Δt . One frequency (Ka) was selected for its poor snow penetration to ensure the signal is backscattered as close to the snow surface as possible, and the second frequency was selected to reflect as close to the snow-ice interface or snow-ground interface as possible. Through well established relationships of refractive index n and snow density ρ , eq. 5 [24] [25], the mission will thus be able to directly measure SWE. The refractive index can be calculated from snow density [24]. This principle has been proven through both ground based studies [20] and the ERS-1 experiment [15].

$$n^2 = 1 + 1.7\rho + 0.63\rho^2 \quad (5)$$

4.4. LASER RETRO-REFLECTOR

Due to the scientific vertical accuracy requirement of 0.06 m, it is important that a precise satellite position is maintained. This accuracy requirement is achieved through the use of a Laser Retro-Reflector which can be trained on by SLR (Satellite Laser Ranging) Ground Stations. This technique ensures the satellite position remains within an accuracy of 6 mm and enables precise orbit determination.

4.5. AIRBORN CAMPAIGN

As previously outlined, the penetration of microwave signals varies depending on snow characteristics. For the Ka-band, this is a particular issue when it is used to determine the top surface layer of the snow which could lead to inaccuracies in SWE estimation if the penetration effect is not fully taken into account. However, the changing penetration capabilities show the sensitivity of microwave measurements to e.g. snow density, which can then be exploited. In order to precisely characterise this effect, the mission concept includes coordinated underflights with airborne laser altimetry.

The Land Vegetation and Ice Sensor (LVIS) with a swath width of 2 km, spatial resolution of 20 m and vertical accuracy of 6 cm [4] performed several CryoSat-2 underflights between 2010 and 2014. A similar concept will be applied during the first two winter seasons of the SWEAT mission. Three campaigns are planned in early, middle and late winter, respectively, to cover different snow stages. The precise snow surface measurement from LVIS will lead to a reliable characterization of Ka-band penetration into different types of snow. Flight lines are planned in Greenland, on Arctic sea ice and in tundra regions of Finland. These activities will

be coordinated with dedicated ground campaigns for calibration and validation of SWE retrieval.

5. VALIDATION AND CALIBRATION

5.1. SWE

Dedicated ground campaigns are used for in-situ measurements of SWE, density, snow height or snow microstructure in order to calibrate and validate the SWE retrieval from the dual-frequency altimeter. The additional measurements of snow characteristics will improve the link from the altimeter observations to SWE information. They are done on land as well as on sea ice and in coordination with airborne laser altimetry in order to have a good validation (e.g. CryoVex).

5.2. ALTIMETER

In addition to the internal calibration on board, the calibration and validation for altimeters can be done through active microwave transponders. This method was used for Cryosat [11] or Jason-2 and Envisat altimeters [16]. Thereby the transponders receive the altimeter signal, amplify the signal and send it back to the satellite. By doing this, a well-known reference signal is retrieved to calibrate and validate the altimeter. The SWEAT mission will also use conventional sea surface calibration [27] and cross-calibration with other altimeters.

6. SCIENTIFIC REQUIREMENTS (SR)

For this mission, there are two primary types of surface that SWE measurements will be focused on; the measurement of SWE on (1) sea ice and (2) land. The mission requires a clear list of scientific requirements as these will affect how the measurement of SWE on sea ice and on land are undertaken. The specific scientific requirements are shown in the left column of Figure 5.

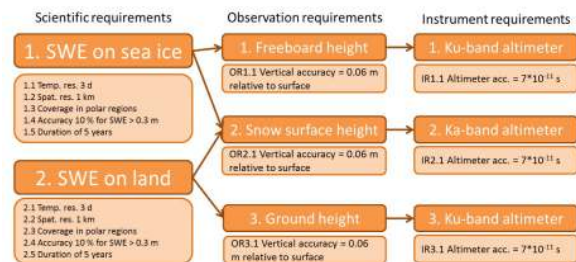


Figure 5: Overview of all requirements.

Due to the dynamic nature of snow in the polar regions, a temporal resolution of 3 - 6 days is necessary to resolve the effects of individual weather events [9] [32]. Therefore, a temporal resolution of 3 days has been selected as the first scientific requirement of this mission so that a detailed observation and analysis of SWE and how it changes can be ascertained.

Due to the year round consistency of snow surface presence in the polar regions, SWEAT will observe snow on land and on sea ice in these areas.

Since snow is not evenly distributed on the Earth's surface in the cryosphere, a high 1 km² resolution is required to ensure good spatial resolution [7] [30]. The required SWE accuracy for SWEAT has been ascertained based on the accuracy requirements for SWE on previously proposed missions such as CoReH2O where accuracy of SWE > 0.3 m equals 10 % and where accuracy of SWE < 0.3 m equals 3 cm.

Because of variability of snow deposition on an annual basis, a final scientific requirement of a lifetime of 5 years has been chosen for the SWEAT mission. By monitoring the changes over several years, the differences can be more clearly recognized for the generation of statistically significant conclusions [7].

The observation requirements determine the vertical accuracy needed on freeboard, snow surface and ground height measurements, as seen in Figure 5. The vertical accuracy is based on the accuracy of measuring SWE (SWE > 0.3 m: 10 % and SWE < 0.3 m: 3 cm). To calculate the required accuracy of the altimeters in terms of signal return time, a worst case scenario of SWE = 0.3 m and density = 500 kg/m³ was assumed. This translates to a relative vertical accuracy of 0.06 m for the snow surface height measurement and ice/ground height measurement.

7. MISSION DESIGN

The scientific case for this mission has been extensively studied with on-Earth experiments. Therefore, it is estimated that Phase 0-/A/B1 [see Fig. 6] will take a maximum of two years for mission analysis and feasibility studies. All payload instruments have extensive space flight heritage so Phases B2/C/D are expected to take a maximum of 5.5 years. Based on this timeline, a launch in 2026 is envisaged, followed by a nominal operations Phase E of 5 years. In case the mission should not be extended, the disposal scenario will come into place. As Space Situational Awareness is of importance to the SWEAT mission, the spacecraft is designed to deorbit within 5 years to reduce the space debris. This will

be achieved by performing a burn maneuver to move from the circular target orbit to an elliptical, 460 km perigee orbit and deorbit within 5 years. The timeline of the SWEAT mission is depicted in Figure 6.

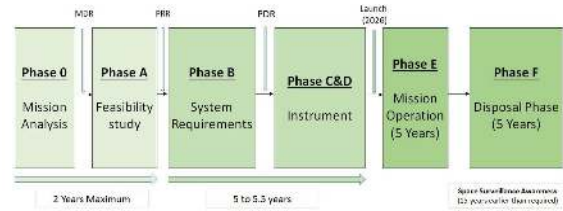


Figure 6: The timeline of the SWEAT mission.

7.1. TARGET ORBIT

In order to fulfill the scientific requirements 1.1 and 2.1, a target orbit with a revisit time of 3 days is needed. In addition, a large Earth surface coverage area in the polar regions is required (SR 1.3). Table 1 states the specifications of the target orbit, which guarantees a repeating orbit as well as a 13.2 % coverage within the area of interest.

Table 1: Orbit specification

Altitude	761.4 Km
Eccentricity	0 (circular)
Inclination	90 °
Orbital period	100.1 min
Eclipse ratio	35 %

8. SATELLITE DESIGN

8.1. PAYLOAD DESCRIPTION

Based on the observation requirements of this SWEAT mission, the payload proposed should be composed of the following: Two dual-frequency Ka-band (35 GHz) and Ku-band (13.5 GHz) altimeter instruments (Table 1). One Laser Retro-Reflector (LRR).

8.2. STRUCTURES AND MECHANISMS

The satellite structural envelope is based on the CryoSat design and is illustrated in diagrammatic form in Figure 7.

Table 2: Two dual-frequency Ka-band (35 GHz) and Ku-band (13.5 GHz) altimeter instruments

Instrument	Ka-band altimeter	Ku-band altimeter
Mass (kg)	45	49
Power / Output power (W)	75 / 2	149 / 25
Data rate (kbits/s)	43	12
Pulse Range Frequency (PRF) (kHz)	4	17.8
Pulse Length (us)	110	50
Bandwith (MHz)	500	320
Thermal operating range (C)	-40 to +85	-35 to -5
Signal-to-noise ratio	>10 dB	>10 dB

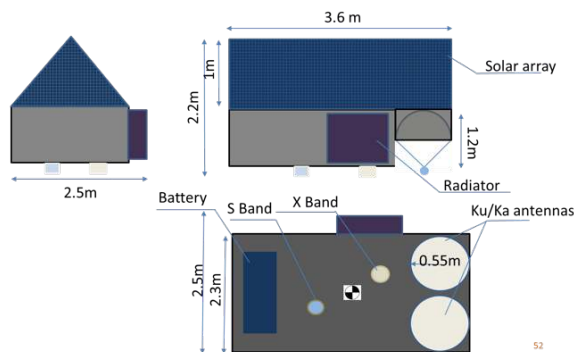


Figure 7: Spacecraft design

The structure and mass of the satellite determines the launch vehicle required. To keep the mass to a minimum, the satellite frame and honeycomb panels will be made of aluminum. The satellite does not have any deployable mechanisms to reduce the risk.

8.3. THERMAL CONTROL SYSTEM

Two elements on board the spacecraft are identified as temperature sensitive: the payloads and the batteries. The operating temperature of the payloads used is between $-35\text{ }^{\circ}\text{C}$ and $-5\text{ }^{\circ}\text{C}$, the cooling is achieved by using passive elements like radiators, heat pipes and louvres. The batteries have an optimal power efficiency between $20\text{ }^{\circ}\text{C}$ and $40\text{ }^{\circ}\text{C}$ and are therefore equipped with active heaters.

8.4. ALTITUDE & ORBIT CONTROL

The satellite payloads require a spatial resolution of 1 km and a pointing accuracy of 0.01° . This is because the orientation of the interferometric baseline needs to be very accurately measured in-flight especially in the roll-axis. Even small errors in the satellite roll-angle translate into substantial errors for the elevation measurements at the off-nadir points. To mitigate these, the spacecraft will utilize 3-axis stabilization and maintain an autonomous inertial attitude determination and

control. The satellite therefore will have an array of different attitude sensors including: three star trackers (in cold redundancy), sun sensor, three-axis magnetometer, GPS/Galileo unit and laser retro-reflectors to fulfil the scientific requirements. Three magnetorquers, four momentum wheels (one cold redundant) and six thrusters are used for attitude control. The polar nature of the orbit implies that the beta angle will change on a continual basis, which determines the degree of orbital eclipse time an object experiences and gives us information about the position of the Sun with respect to the satellite. To ensure the radiator, which is responsible for maintain the payload temperature range, is pointing deep space and is not facing the Sun, the satellite will undertake a 180° yaw maneuver periodically using the momentum wheels.

Regarding the end-of-life scenario, a monopropellant hydrazine thruster ($ISP = 225\text{ m/s}$) was selected due to technological reliability and simplicity characteristics. Due to the exothermic chemistry characteristic, the propulsion system has minimal power requirements. A hydrazine fuel mass of 34 kg (including margins for orbital corrections) is required for the entire mission duration.

8.5. TELEMETRY TRACKING & COMMUNICATION

For the communication between the satellite and the ground station, an S-band transceiver for telecommand upload and telemetry download is used. For downloading the scientific data, an X-band downlink is established to provide higher data rates. As a backup additional UHF-antennas are installed for emergency purposes. The following table lists the main specifications of the nominal links, compared with a suitable ESTRACK ground station, in this case Svalbard(SG-3).

Table 3: S-band and X-band parameters - Svalbard (Norway) Ground Station.

	S-Band up	S-Band down	X-Band down
Frequency Range [GHz]	2.025 - 2.110	2.200 - 2.290	8.025 - 8.400
Data Rate [bit/s]	(64-1024)k	(1024-6250)k	(10-300)M
P_{tx} [W]	5000	2.2	5
E_B/E_N (SG-3)	60.8	29.5	23.3

8.6. POWER SUBSYSTEMS

The satellite has a total power duty cycle requirement of 706 W (including 20 % margin). The solar arrays have been designed to a 20 % efficiency instead of their typical 29 % efficiency to take into account a lower power generation scenario caused by degradation before the end of life.

Assuming a solar flux of 1300 W/h and accounting for the charging needs of the battery system, the optimized panel surface area is 5.43 m². However, SWEAT uses a solar panel surface area of 5.54 m² for each primary panel (pointing Zenith) and 1.17 m² for each secondary panel fitted onto the triangular shaped top of the satellite (13.43 m² in total). One face of the triangular solar array generates 304.2 W of power, which is the amount required to start up and detumble. At points within the 90° polar orbit chosen, only one solar panel face is expected to be illuminated, so each solar panel face has been designed to deal with the power requirements of the entire satellite.

The batteries will require a 110 Ah capacity to ensure the satellite can be powered in the worst case eclipse time while also operating both payloads at peak power. Therefore, two lithium ion batteries are onboard (in cold redundancy), both connected to an unregulated bus and a power system control unit.

8.7. ON-BOARD DATA HANDLING

To cope with the data loading on the satellite, the ERC32 microprocessor with Cryosat heritage has been chosen. The data volume gathered during an orbit is listed in Table 4.

Table 4: Data handling

Ka	192,128 Mbits
Ku	72,048 Mbits
Housekeeping	13, 209 Mbits (5% of all data volume)

The on-board solid state memory is designed to store at least the data volume of 3 orbits without ground station contact, which gives 3.1 GBytes at minimum.

9. GROUND SEGMENT

This mission will use ESA ESTRACK network ground stations, Svalbard (Norway), Troll (Antarctica) and Prince Albert (Canada), as they are located close to the poles for optimal downlink duration. The mission requires a total downlink time every orbit cycle of 15 minutes for the payload data and 3 minutes for housekeeping data. Overall, the satellite has a mean total access time per orbit with these ground stations of 23 minutes. Any data gathered below 60° and above -60° latitudes will not be transmitted.

10. LAUNCH SEGMENT

Vega can lift a volume of 41.84 m³ in a cylinder with a 2.6 m diameter, a 7.88 m height and a payload mass of 1430 kg, therefore it is suitable for launching the SWEAT satellite. Since the SWEAT satellite has a total mass of 843 kg and a dimension of 3.6 × 2.5 × 2.2 m³ (length/ width/ height), the satellite fits with spare room for further secondary payloads.

11. RISK ASSESSMENT

The TRL of the radar altimeters is low and this increases the risk, however the same frequencies have been flown at different orbits and one specialist company, Alenia Space, has a good track record with radar altimetry missions such as CryoSat and Jason-1. The major risks can be seen in Figure 8.

Event	Severity	Likelihood	Total Risk	Mitigation
Obsolescence	3	B	6	Longer phase 0-A-B1
Something not built to specifications	3	B	6	Severity could range from development delays to impaired data gathering
AOCS fails	4	B	8	Redundant system
Development of hydrological models reduce scientific value	4	A	4	No known missions are currently planned to investigate SWE in the same way as SWEAT

Figure 8: Risk assessment.

12. COST

Table 5: Mission component costs and total costs

Item	Costs (Mil €) condition 2016
(Instrument development (before start))	15
Industrial costs spacecraft (Heritage Cryosat)	100
Payload	80
Vega Launcher	45
Scientific data processing (high data rating processing intensive)	35
Operational cost	45
Airplane campagne	1
Project Team (10% of industrial costs + scientific data processing + operational costs)	25
Contingency (15 % of industrial costs + scientific data processing + operational costs + project team)	43
Overall costs	389

13. CONCLUSION

SWE is very important in hydrological and climate processes. The SWEAT mission will measure SWE directly from space at a high spatiotemporal resolution. The mission will generate data which will improve current SWE products using a novel technological combination of Ku- and Ka- band radar altimeters.

REFERENCES

- [1] Barnett, T.P. et al (2005). Potential impacts of a warming climate on water availability in snow-dominated regions. *Nature*.
- [2] Beaven, S. G. et al. (1995). Laboratory measurements of radar backscatter from bare and snow-covered saline ice sheets. *Remote Sensing*.
- [3] Bernier, P. Y. (1987). Microwave remote sensing of snowpack properties: potential and limitations. *Hydrology Research*.
- [4] Blair, B. et al. (2011). Mapping Land, Vegetation, and Ice with Wide-swath, Full-waveform Laser Altimetry from High-altitude UAV Aircraft. *American Geophysical Union*.
- [5] Durand, M., and Liu, D. (2012). The need for prior information in characterizing snow water equivalent from microwave brightness temperatures. *Remote Sensing of Environment*.
- [6] Dutra, E et al. (2010). An improved snow scheme for the ECMWF land surface model: description and offline validation. *Journal of Hydrometeorology*.
- [7] ESA (2012). Report for Mission Selection: CoReH2O, ESA SP-1324/2.
- [8] ESA (2014). Geophysical Correction Application in Level 2 CryoSat Data Products.
- [9] ESA (2015). ESA-GEWEX. Earth Observation and water cycle science priorities.
- [10] Foresta, L. et al. (2014). Fine Ice Sheet margins topography from swath processing of CryoSat SARIn mode data. *EGU General Assembly Conference Abstracts*.
- [11] Fornari, M. et al. (2013). Cryosat SIRAL Calibration and Performance. *Geophysical Research Abstracts*.
- [12] Foster, J.L. et al.(2005). Quantifying the uncertainty in passive microwave snow water equivalent observations. *Remote Sensing of Environment*.
- [13] Furtado, J. C. et al. (2015). Eurasian snow cover variability and links to winter climate in the CMIP5 models. *Climate Dynamics*.
- [14] Gray, L. et al. (2013). Interferometric swath processing of Cryosat data for glacial ice topography. *The Cryosphere*.
- [15] Guneriusson, T. (2001). InSAR for estimation of changes in snow water equivalent of dry snow. *IEEE Transactions on Geoscience and Remote Sensing*.
- [16] Hausleitner, W. et al. (2012). A New Method of Precise Jason-2 Altimeter Calibration Using a Microwave Transponder. *Marine Geodesy*.
- [17] Hensley, S. et al. (2015). Interferometric penetration into dry snow and sea ice at Ka-band. In *Synthetic Aperture Radar (AP SAR)*.
- [18] Heymsfield, A. J. and Miloshevich, L. M. (2003). Relative humidity and temperature influences on cirrus formation and evolution: Observations from wave cloudIIs and FIRE II. *Journal of the atmospheric sciences*.
- [19] IPCC (2014). *Climate Change 2014: Synthesis Report*.
- [20] Leinss, S. et al. (2015): Snow Water Equivalent of Dry Snow Measured by Differential Interferometry. *IEEE Journal of Selected Topics in Applied Earth Observations and Remote Sensing*.
- [21] Oerlemans, J. (2001). *Glaciers and Climate Change*. CRC Press.
- [22] Pulliainen, J. and Hallikainen, M. (2001). Retrieval of regional snow water equivalent from space-borne passive microwave observations. *Remote sensing of environment*.
- [23] Pulliainen, J. (2006). Mapping of snow water equivalent and snow depth in boreal and sub-arctic zones by assimilating space-borne microwave radiometer data and ground-based observations. *Remote sensing of Environment*.
- [24] Maetzler, C. (1987). *Applications of the Interaction of Microwaves with the Seasonal Snow Cover*. *Remote Sensing Reviews*.
- [25] Maetzler, C. (2006). *Thermal Microwave Radiation: Applications for Remote Sensing*, Chapter 5, Microwave dielectric properties of ice. *IET Electromagnetic Waves Series*, Stevenage, U.K.
- [26] McEvoy, A. et al. (2003). *Practical handbook of photovoltaics: fundamentals and applications*. Elsevier.
- [27] Mitchum, G. T. (2000). An improved calibration of satellite altimetric heights using tide gauge sea levels with adjustment for land motion. *Marine Geode*
- [28] Moller, D. et al. (2011). The Glacier and land ice surface topography interferometer: An airborne proof-of-concept demonstration of high-precision ka-band single-pass elevation mapping. *IEEE Transactions on Geoscience and Remote Sensing*.
- [29] Mueller, K. (2011). *Microwave penetration in polar snow and ice: Implications for GPR and SAR*. PhD Thesis, University of Oslo.
- [30] National Research Council (NRC), Committee on Earth Science and Applications from Space, Richard A. A., and Moore, B. (2007): *Earth science and applications from space: National imperatives for the next decade and beyond*. National Academies Press.
- [31] National Snow Ice Data Center (2016), AMSR-E/Aqua-Data, Data Uncertainty, <https://nsidc.org/data/amsr/data-quality/data-uncertainty.html>, retrieved July 20, 2016
- [32] Nghiem, S. and Tsai, W. (2001): Global snow cover monitoring with spaceborne Ku-band scatterometer. *IEEE Trans. Geosci. Remote. Sens.*
- [33] Randall, D. A., et al. (2007). *Climate models and their evaluation*. In *Climate change 2007: The physical science basis*. Cambridge University Press.
- [34] Rignot, E. et al. (2001). Penetration depth of interferometric synthetic-aperture radar signals in snow and ice. *Geoph*
- [35] Strozzi, T. (1996). Backscattering measurements of snowcovers at 5.3 and 35 ghz. *Universitat Bern*.
- [36] Sturm, M. et al. (2010). Estimating Snow Water Equivalent Using Snow Depth Data and Climate Classes. *Journal of Hydrometeorology*. Res. Lett.
- [37] Thackeray, C. W. et al. (2015). Quantifying the skill of CMIP5 models in simulating seasonal albedo and snow cover evolution. *Geophy*
- [38] Ulaby, F. T. et al. (1981). *Microwave remote sensing: from theory to applications*. Artech House.
- [39] United States Department of Agriculture (2016), What is Snow Water Equivalent? http://www.nrcs.usda.gov/wps/portal/nrcs/detail/or/snow/?cid=nrcs142p2_046155, retrieved July 20, 2016
- [40] Verron, J. and Steunou, N. (2006). *AltiKa: A micro-satellite Ka-band altimetry mission*. *ESA Special Publication*.
- [41] Vincent, P. et al. (2006). *AltiKa: A Ka-band altimetry payload and system for operational altimetry during the GMES period*. *Sensors*.
- [42] Wingham, D. J. et al. (2006). *CryoSat: A mission to determine the fluctuations in Earth's land and marine ice fields*. *Advances in Space Research*.